Journal of Pharmaceutical Sciences 111 (2022) 2531–2539

Contents lists available at ScienceDirect

Journal of Pharmaceutical Sciences

journal homepage: www.jpharmsci.org

Pharmaceutics, Drug Delivery and Pharmaceutical Technology

Preparation and Characterization of Platelet Lysate (Pl)-Loaded Electrospun Nanofibers for Epidermal Wound Healing

Simin Nazarnezhad[a], Farzad Kermani[b], Vahid Reza Askari[c,f], Seyede Atefe Hosseini[d], Alireza Ebrahimzadeh-Bideskan[e,f,*], Ali Moradi[g], Reza Kazemi Oskuee[d,f], Sahar Mollazadeh[b], Saeid Kargozar[a,*]

[a] Tissue Engineering Research Group (TERG), Department of Anatomy and Cell Biology, School of Medicine, Mashhad University of Medical Sciences, Mashhad 917794-8564, Iran
[b] Department of Materials Engineering, Faculty of Engineering, Ferdowsi University of Mashhad (FUM), Azadi Sq., Mashhad 917794-8564, Iran
[c] Department of Pharmaceutical Sciences in Persian Medicine, School of Persian and Complementary Medicine, Mashhad University of Medical Sciences, Mashhad, Iran
[d] Department of Medical Biotechnology and Nanotechnology, Faculty of Medicine, Mashhad University of Medical Sciences, Mashhad, Iran
[e] Department of Anatomy and Cell Biology, School of Medicine, Mashhad University of Medical Sciences, Mashhad, Iran
[f] Applied Biomedical Research Center, Mashhad University of Medical Sciences, Mashhad, Iran
[g] Orthopedic Research Center, Mashhad University of Medical Sciences (MUM), Mashhad, Iran

ARTICLE INFO

Article history:
Received 2 February 2022
Revised 11 April 2022
Accepted 11 April 2022
Available online 17 April 2022

Keywords:
Electrospun nanofibers
Nanocomposite
Chitosan
Poly(ε-caprolactone)
Gelatin
Poly (vinyl alcohol)
Platelet lysate (PL)
Wound healing

ABSTRACT

Skin defects are among the most prevalent and serious problems worldwide; it is necessary to provide appropriate coverage in order to reduce possible mortality risk and accelerate wound healing. In this study, we have designed a series of extracellular matrix (ECM)-mimicking nanofibrous scaffolds composed of both natural (gelatin (GEL) and chitosan (CS)) and synthetic (poly(ε-caprolactone) (PCL) and poly (vinyl alcohol) (PVA)) polymers. The 3D constructs (PCL/GEL-PVA/CS) were reinforced with 5% (w/w) of platelet lysate (PL) for promoting cells viability and mobility. The physicochemical characterizations of nanofibers confirmed suitable hydrophilicity, controlled degradability, and water uptake of 250.31 ± 62.74%, and 222.425 ± 86.37% for the PCL/GEL-PVA/CS and PCL/GEL-PVA/CS + PL nanofibers, respectively. The scanning electron microscopy (SEM) images exhibited the mean diameter of the fabricated fibers (PCL/GEL-PVA/CS) in the range of 454 ± 257 nm. The blended samples (PCL/GEL-PVA/CS) were also confirmed to have higher ultimate tensile stress (UTS) (3.71 ± 0.32 MPa). From a biological point of view, the fabricated scaffolds showed appropriate blood compatibility and great potential to avoid bacterial invasion. Altogether, the tailored fabrication of PCL/GEL-PVA/CS nanofibers may be considered a suitable construct for epidermal wound healing.

Introduction

Skin is the largest organ of the human body, which serves as a protective barrier against external damages including thermal, chemical, and mechanical injuries. Furthermore, besides preventing bacterial invasion and infection, skin plays a pivotal role in maintaining the body hemostasis, thermoregulation, and providing a moist environment that inhibits dehydration.[1] This tissue is at the risk of diverse damages and injuries, ranging from acute (e.g., burns) to chronic (e.g., diabetic ulcers) wounds. The epidermis, the outermost layer of skin, is generally ruptured after any injuries, threatening the human body against pathogens and other life-threatening agents. Therefore, providing a provisional matrix capable of maintaining water content, exhibiting anti-bacterial properties, and supporting cell behaviors (recruitment, migration, attachment, and proliferation) is of utmost importance in regenerative medicine strategies.

Electrospun nanofibers have emerged as promising three-dimensional (3D) scaffolds for managing skin wounds. These constructs display some physico-chemical, mechanical, and biological characteristics in favor of skin repair and regeneration, including (I) imitating the ECM structure; (II) possessing a high surface-to-volume area; (III) removing excessive exudates from the wound bed; (IV) preventing the bacteria infiltration into the wound bed; and (V) providing a provisional substrate for cell adhesion, proliferation, and differentiation. All the mentioned properties could positively affect re-epithelialization, tissue formation, and vascularization at injured regions.[2] In addition, it is feasible to incorporate various bioactive molecules (e.g.,

* Correspondence
E-mail addresses: askariv@mums.ac.ir, vahidrezaaskary@gmail.com (V.R. Askari), EbrahimzadehBA@mums.ac.ir (A. Ebrahimzadeh-Bideskan), kargozarsaeid@gmail.com (S. Kargozar).

https://doi.org/10.1016/j.xphs.2022.04.008
0022-3549/

growth factors (GFs)) into electrospun nanofibers to improve their biological performance. Up to date, huge numbers of natural and synthetic polymers have been successfully used for the preparation of electrospun nanofibers.[3] Chitosan, a naturally occurring biopolymer, is commonly being used for skin tissue engineering due to its proper biocompatibility, biodegradability, antibacterial activity, and hemostatic properties.[4] However, it is not possible to use chitosan for the preparation of electrospun nanofibers without its combination with other polymers like poly(vinyl alcohol) (PVA). PVA is a food and drug administration (FDA)-approved polymer for biomedical utilities, which possesses good cytocompatibility, biodegradability, as well as appropriate strength and elongation capability.[5] Having an appropriate mechanical strength, poly(caprolactone) (PCL) has been applied as one of the main building blocks of scaffolds designed for skin tissue engineering.[6] Nevertheless, the lack of cell-recognition sites and the hydrophobic nature of PCL result in poor cell adhesion and proliferation. To overcome this limitation, PCL can be blended with various natural biopolymers such as gelatin (GEL). GEL is derived by the partial hydrolysis of collagen and is being extensively used for skin tissue engineering applications thanks to its biocompatibility, biodegradability, affordability, and low immunogenicity.[7]

During the normal process of wound healing, different kinds of GFs and cytokines are required for accelerating skin tissue repair and regeneration. Platelet lysate (PL) represents a rich source of different bioactive molecules (e.g., platelet-derived GF (PDGF), vascular endothelial GF (VEGF), epidermal GF (EGF), fibroblast GF (FGF), and tumor necrosis-alpha (TNF-α)) and is being widely applied for managing soft tissue injuries.[8] Indeed, PL can accelerate cutaneous wound healing by promoting keratinocytes' migration, fibroblasts' proliferation, and activating inflammatory responses.[9,10] Previously reported experiments have demonstrated that the therapeutic efficacy of PL is higher than a single dose of any GF administration.[11] Accordingly, PL has gained much attention in skin tissue engineering strategies and is being currently incorporated into tissue-engineered (TE) constructs to provide a prolonged release of GFs and cytokines for improving cutaneous tissue healing.

In the present study, we developed a series of electrospun nanocomposites made of PVA/CS and PCL/GEL containing PL for the potential use in epidermal regeneration. In this regard, the potential of the electrospun scaffolds was assessed in terms of loading and release of PL, and consequent effects in mammalian cells' behaviors (viability, proliferation, and migration). Freeze-dried PL was incorporated into the PVA/CS polymeric solution for improving the biological properties of the final construct. A complete set of physico-chemical, mechanical, and biological assays were carried out to uncover the real potential of the PL-incorporated electrospun nanocomposites in treating skin wounds (e.g., burns). The obtained data demonstrate a bright future of bioactive molecules containing electrospun mats, as provisional substitutes, for managing acute epidermal wounds.

Materials and Methods

Isolation and Activation of PL

Fifteen Wistar rats were randomly selected and used for the isolation of PRP through a two-step centrifugation process. First, the whole blood of the animals was collected into sterile citrated tubes (A191237B, Greiner Bio-One, Australia) and centrifuged at 1200 rpm for 20 minutes. This process resulted in the formation of three distinct layers, including the supernatant or platelet-poor plasma (PPP), the PRP containing buffy coat in the middle, and the erythrocytes at the bottom. The platelet counts were 629 $\times$ 10^3/uL in the PRP samples. The PRP was then transferred into microtubes and underwent the second centrifugation at 2500 rpm for 15 minutes. The samples were stored at -20°C for further utilization. For platelet activation, the samples were thawed and immersed in liquid nitrogen for 1 minute followed by incubating in the water bath at 37°C for 6 minutes. This process was repeated 3 times and the samples were further centrifuged at 9000 $\times$ g for 3 minutes. The supernatant, i.e., PL, was then transferred to new microtubes and finally freeze-dried for 24 h.

Fabrication of Electrospun Nanofibers

A 10% w/v solution of PCL (MW$\sim$ 80.000, cat#440744) and GEL (cat#G2500) was separately prepared by dissolving in trifluoroethanol (TFE) (cat#T63002) and stirred overnight at room temperature. For the blended polymeric system, the PCL solution was mixed with the GEL solution in a ratio of 50:50. Then glacial acetic acid (2% v/v) was added to the blended solution to avoid phase separation during the electrospinning process. On the other side, the PVA/CS blends with a ratio of 70:30 (PVA:CS) were prepared by adding PVA (cat#8.43866) solution (10% w/v in water) to CS (low molecular weight, degree of deacetylation 75–85%, cat#448869) solution (3% w/v in 2% acetic acid). (All the polymers and solvents were purchased from Merck, Germany). Prior to the electrospinning, the freeze-dried PL was added to the PVA/CS polymeric system at concentrations of 2, 5, 10, and 20 % of the polymer weight. The electrospinning machine having two distinct syringe pumps (Nano Azma, Iran) was utilized for fabricating nanofibrous mats. The feeding rate was set as 1mL/h for each pump. The polymer solutions were jet from the tip of a 22-gauge blunt needle to the grounded collector at the distance of 15 cm between the needle tip to the collector. A voltage of 15 kV was applied for each polymer solution using a high-voltage power supply. The obtained nanofibers were crosslinked overnight by exposing them to 0.5% glutaraldehyde vapor.

Characterization of Electrospun Nanocomposites

Scanning Electron Microscopy

The shape and the morphology of the nanofibers were evaluated using field emission scanning electron microscopy (FESEM) (MIRA3 TESCAN, Czech Republic). The average diameter of the nanofibrous mats was quantified by Image J software (NIH, USA).

Fourier Transform Infrared Spectroscopy (FTIR)

The functional groups of the prepared electrospun nanofibers were investigated by using a conventional FTIR Spectrometer (NICOLET IS10 FT-IR SPEC, Thermo Fisher, USA). The FTIR spectra were collected over the range of 400-4000 cm^{-1} with a resolution of 4 cm^{-1} and the number of scans 16.

Mechanical Evaluation

The mechanical properties of the prepared mats were evaluated by a universal testing machine (UTM) (SANTAM STM, Iran). For this aim, the samples were cut into 1 $\times$ 7 cm^2 rectangles and fixed between the grips of the instrument. A rate of 0.5 mm/min was applied to stretch the nanofibers in the axial direction. The tensile strength, Young's modulus, and the ultimate tensile strain (UTS) at breaking were quantified using a stress-strain curve.

Contact Angle Analysis

The hydrophobicity of the fabricated nanofibers was measured by a contact angle measurement system (Adeeco, Iran). Droplets with the volume of 2μL were dropped onto the surface of nanofibrous membranes (PCL/GEL, crosslinked PVA/CS (c-PVA/CS), cross-linked PCL/GEL-PVA/CS (c-PCL/GEL-PVA/CS), and cross-linked PCL/GEL-PVA/CS + PL (c-PCL/GEL-PVA/CS + PL)) and images were captured after 1, 2, and 5 seconds.

Swelling Test

The water uptake ratio of the nanofibrous mats was evaluated by a swelling test. To do this, the electrospun nanofibers were first cut (1×1 cm^2), weighed, and immersed in phosphate-buffered saline (PBS). After 24 h, the samples were removed from PBS and gently placed on filter paper to take away the excess water. The samples were then weighed again, and the degree of swelling was calculated using the following formula:

$$\text{Degree of swelling}(\%) = [(W_1 - W_0)/W_0] \times 100$$

Here, W_0 is the dry weight of the samples before the immersion in PBS, and W_1 is the wet weight of the samples after soaking in PPB.

Weight Loss Analysis

For evaluating the weight loss, the nanofibrous scaffolds were first cut (1×1 cm^2) and weighed. Then the samples were soaked in PBS and incubated at 37°C for 28 days. The samples were removed from BPS and dried at 1, 4, 7-, 14-, 21-, and 28-days post-incubation. The weight loss (%) was calculated according to the following formula:

$$\text{Weightloss}(\%) = [(W_1 - W_0)/W_0] \times 100$$

where the W_0 and W1 represent the dry weight of the samples before and after immersion in PBS, respectively.

Protein Release Profile

The release of PL from the nanofibrous mats was measured by a quantitative standard method, i.e., the BCA protein assay. For this purpose, the nanofibrous mats with and without PL (1×1 cm^2) were soaked in 1 mL PBS and then incubated at 37°C. At different time points (6 h and 1, 3, 7, 14, 21, and 28 days), the cumulative release rate of total protein from the scaffolds to PBS was recorded using the BCA kit (Takara, Japan) according to the manufacturer's instructions.

Biological Evaluation of Fabricated Nanofibers

Cell Viability Assay

The mouse embryonic fibroblast cell line NIH/3T3 was cultured in high glucose Dulbecco's Modified Eagle Medium (DMEM) (Gibco, US) supplemented with 10% (v/v) fetal bovine serum (FBS) (Gibco, US) and 1% (v/v) antibiotic (complete medium) at 37°C in a humidified atmosphere of 5% CO_2. The medium was changed every 2 days and the cells were sub-cultured at a confluence of 70%. Nearly 3×10^3 of the NIH/3T3 cells were seeded in a 96-well plate (SPL life science, South Korea) and incubated overnight. Then the UV-sterilized nanofibrous mats were added to the cultures and incubated for 24, 48, and 72h. After the incubation times, 10 μL of 3-(4,5-dimethylthiazol-2-yl)-2,5-diphenyltetrazolium bromide (MTT) solution was added to each well and further incubated for another 4h. Thereafter, all cell culture media was gently removed and 100 μL of dimethyl sulfoxide (DMSO) was added to each well and incubated for 20 min. Finally, the rate of cell proliferation was determined via measuring the absorbance of each well at wavelengths of 570 nm and 690 nm using a microplate reader (Epoch, Bio Tek, US).

Cell Adhesion

The NIH/3T3 cells (2×10^4) were seeded on the nanofibrous mats and incubated for 4 days. After completing the incubation, the cell/samples constructs were fixed with glutaraldehyde (2.5% v/v) for 24h, followed by rinsing with deionized water and dehydration in sequential concentrations (30, 50, 70, 75, 80, 85, 90, 95, and 100%) of ethanol. Eventually, the samples were freeze-dried and surface-coated with gold (Edwards's coating system E306A) to detect cell adhesion under SEM.

Cell Migration (Scratch Assay)

The cell migration assay was performed according to Ref. 12. In brief, human umbilical cord vein endothelial cells (HUVECs) at a density of 2×10^4 were seeded in 12-well culture plates and incubated overnight. The cell monolayer was scraped by a 100 μL pipette tip in a straight line, and the cell culture medium was immediately replaced. The UV-sterilized electrospun nanofibers were added to the wells and incubated for 6, 12, 24, and 48h. At the time intervals, the scaffolds were removed, and the rate of cell migration was acquired by capturing images and further quantification by using Image J software (National Institutes of Health, US).

In vitro *Blood Compatibility Assay*

For evaluating the hemocompatibility of the fabricated nanofibers, the samples were punched and put into the 96-well plates. The human whole blood was first isolated and anticoagulated. Then 200 μL of the whole blood was added to the plates, followed by incubation at 37 °C for 60 min. Blood diluted in deionized water and normal saline were regarded as positive and negative controls, respectively. The samples were then centrifuged at 1500 rpm for 10 min, and the absorbance of supernatants was read at 545 nm. The degree of hemolysis was calculated using the following formula

$$\text{Degree of hemolysis}(\%) = \left[(D_s - D_n)/(D_p - D_n)\right] \times 100$$

Where D_s, D_p, and D_n represent the absorbance of samples, the positive control, and the negative control, respectively.

Bacterial Penetration Properties

In addition, to evaluate the potential of nanofibers for preventing bacterial invasion, glass test tubes containing 5 mL of LB broth were covered by the electrospun nanofibers (test area: 0.8 cm^2). The open tubes and tubes sealed with the cotton ball were considered as positive and negative controls, respectively. The tested tubes were maintained at ambient conditions for 3 and 7 days, and the absorbance of samples was read at 600 nm. The cloudiness of the mixture in any tube indicates bacterial contamination.

Statistical Analysis

All the experiments were carried out as triplicates. All statistical analysis was performed by GraphPad Prism (v9.0). A two-way ANOVA followed by Tukey's test was performed. To compare the mechanical data of nanofibers, a t-test was utilized. A P-value of 0.05 was considered significant for all data. All graphs are presented as mean +/− standard error of the mean (SEM).

Results

Physico-Chemical and Mechanical Properties

Surface Morphology of Nanofibers

The SEM micrographs of the fabricated nanofibers are shown in Fig. 1. As it can be seen, the mats have a uniform distribution and bead-free structure with randomly oriented nanofibers and open interconnected porosity. The average diameter of the fabricated nanofibrous mats is represented in Table 1.

FTIR Spectroscopy

The chemical structure of the nanofibrous mats was evaluated by FTIR spectroscopy, and the results are shown in Fig. 2. Regarding the data, the observed broad peak of absorption at 3300 cm^{-1} may be related to a hydroxyl group (O—H) stretching. In addition, the absorption bands at 600-700, 940-980, 1000-1320, 1500-1600, 1695-

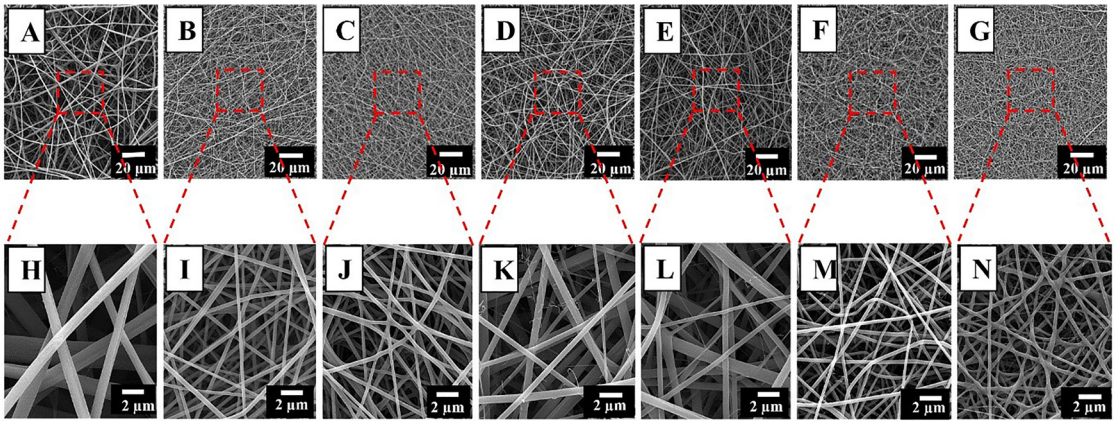

Figure 1. FESEM micrographs of PCL/GEL (A and H), PVA/CS (B and I), c-PVA/CS (C and J), PCL/GEL-PVA/CS (D and K), c-PCL/GEL-PVA/CS (E and L), PCL/GEL-PVA/CS + PL (F and M), and c-PCL/GEL-PVA/CS + PL (G and N).

1705, and 2800-2950 cm^{-1} are attributed to C—H and N—H, N—O, C—O, N=O, C=O, and CH_2 groups, respectively.

Mechanical Properties of the Electrospun Nanofibers

The mechanical assessment of the fabricated nanofibrous mats revealed that the c-PCL/GEL-PVA/CS group has the highest Young's modulus (6.13 ± 0.83 MPa), while the lowest values (0.57 ± 0.7 MPa) were recorded for the PVA/CS group. The ultimate tensile strength (UTS) of the nanofibrous mats was in the range of 0.69 ± 0.1 MPa to 3.71 ± 0.32 MPa (the PVA/CS and c-PCL/GEL/PVA/CS groups, respectively). The detailed information is shown in **Fig. 3** and Table 2.

Contact Angle

The contact angle values recorded for the prepared nanofibrous scaffolds are depicted in Fig. 1 Supplementary. As shown, PCL/GEL membrane had a water contact angle of 133°, while the other mats, including c-PVA/CS, c-PCL/GEL-PVA/CS, and c-PCL/GEL-PVA/CS + PL, could adsorb all the water, leading to record a contact angle of 0° after 5 seconds post-dropping.

Swelling and Weight Loss

Fig. 4 shows the results of the swelling and dissolution rate of the nanofibrous mats after being incubated in PBS. According to Fig. 4A, water absorption (swelling) values recorded for the PCL/GEL, PVA/CS, PCL/GEL-PVA/CS and PCL/GEL-PVA/CS + PL are 201.5 ± 60.25%, 259.875 ± 68.72%, 250.31 ± 62.74%, and 222.425 ± 86.37%, respectively.

Fig. 4B shows the weight loss of the synthesized nanofibers after 1, 3, 7, and 14, 21, and 28 days of soaking in PBS. The weight loss values were 31.823 ± 1.467, 37.85 ± 1.447%, and 62.377 ± 1.51% for the PCL/GEL, PCL/GEL-PVA/CS, and PCL/GEL-PVA/CS + PL nanofibrous scaffolds on day 28 post-immersion in PBS, respectively.

Table 1
Morphological Properties of Nanofibrous Membranes.

Sample	Mean Diameter (nm)	Thickness (μm)
PCL/GEL	1134 ± 314	96.6 ± 12.25
PVA/CS	279 ± 50	21.6 ± 1.69
c-PVA/CS	270 ± 59	20 ± 1.63
PCL/GEL-PVA/CS	454 ± 257	86 ± 12.96
c-PCL/GEL-PVA/CS	531 ± 258	70 ± 8.165
PCL/GEL-PVA/CS + PL	236 ± 43	45 ± 6.342
c-PCL/GEL-PVA/CS + PL	240 ± 80	51 ± 6.68

Protein Release Assay

The release kinetics of PL from the nanofibrous membranes was evaluated by BCA assay. Based on the obtained data (Fig. 5), a cumulative release of 85.8±5.659, 111.283±6.88, 188.357± 9.163, 201.507±3.662, 211.24±3.945, 226.56±12.391, and 244.28±12.311 μg/mL of PL was observed after 6 h, 1, 3, 7, 14, 21, and 28 days of immersion in PBS, respectively. It should be mentioned that these amounts were obtained after subtracting the concentration of dissolved nanofiber materials from the PL-containing nanofibrous mats.

Biological Properties of Nanofibrous Mats

Cytocompatibility Assessment

The effects of the nanofibers on the viability of NIH 3T3 cells were assessed by MTT assay and represented in Fig. 6 A. Regarding the data, the viability of cells was significantly increased after 48 h incubation with the 5 and 10% PL- containing nanofibrous membranes (120.793 ± 5.443% and 120.860 ± 4.277%, respectively) ($p < 0.05$). It should be stated that no significant changes in the cell viability were observed in the different groups over the other time points.

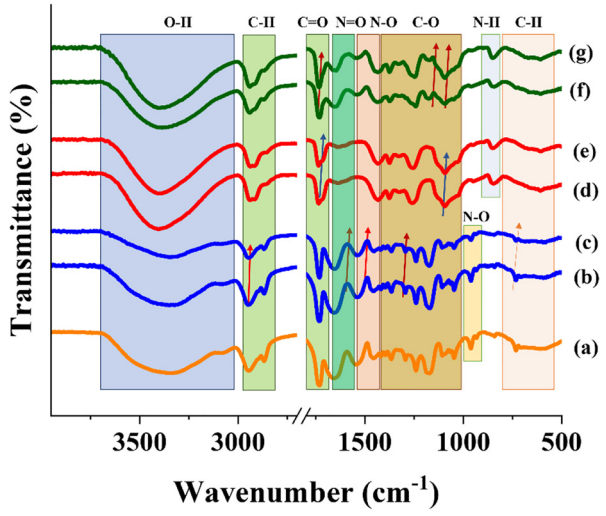

Figure 2. FTIR spectra of PCL/GEL (a), PVA/CS (b), c-PVA/CS (c), PCL/GEL-PVA/CS (d), c-PCL/GEL-PVA/CS (e), PCL/GEL-PVA/CS + PL (f), and c-PCL/GEL-PVA/CS + PL (g).

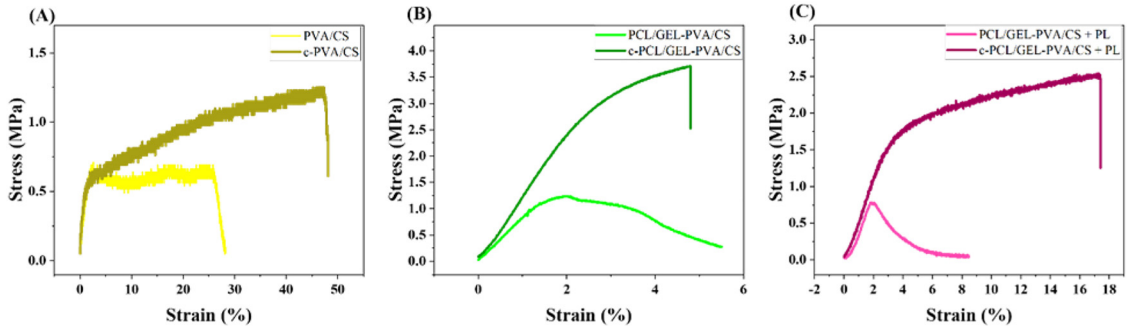

Figure 3. Stress-strain curves of PVA/CS, c-PVA/CS (A), PCL/GEL-PVA/CS, c-PCL/GEL-PVA/CS (B), PCL/GEL-PVA/CS + PL, and c-PCL/GEL-PVA/CS + PL (C).

Table 2
Mechanical Properties of Nanofibrous Membranes.

Composition	Ultimate Tensile Stress (UTS) (MPa)	Failure Strain (%)	Young's Modulus (E) (MPa)
PVA/CS	0.69 ± 0.10	24.8 ± 1.27	0.57 ± 0.7
c-PVA/CS	1.25 ± 0.11	47.27 ± 1.96	0.85 ± 0.6
PCL/GEL-PVA/CS	1.23 ± 0.14	2.1 ± 0.39	3.6 ± 0.7
c-PCL/GEL-PVA/CS	3.71 ± 0.32	4.7 ± 0.76	6.13 ± 0.83
PCL/GEL-PVA/CS + PL	0.77 ± 0.10	2.1 ± 0.11	2.24 ± 0.80
c-PCL/GEL-PVA/CS + PL	2.5 ± 0.16	17.23 ± 0.49	2.76 ± 0.44

Cell Adhesion

The FE-SEM micrographs (Fig. 6 B) exhibit that mouse embryonic fibroblasts (NIH 3T3 cell line) were well-attached on the surface of the fabricated nanofibrous scaffolds after 5 days of the cell seeding.

Cell Migration

The effects of the prepared nanofibrous mats on HUVEC mobility were evaluated by *in vitro* scratch assay. As shown in Fig. 7, there is no significant improvement in the migration capability of HUVEC treated with the nanofibrous membrane as compared with the untreated counterparts after 24 h (28.33 ± 41.74% *vs.* 37.58 ± 7.86%). However, the incorporation of PL into the nanofibers resulted in a sharp increase in cell mobility in comparison with the control group (40.08 ± 5.68% *vs.* 37.58 ± 7.86%, $p < 0.05$) (Fig. 7B).

Blood Compatibility

Fig. 7 C verifies the blood compatibility of the prepared nanofibrous mats. Compared to the positive control (distilled water), the nanofibrous samples had no significant adverse effects ($p < 0.001$) on hemolysis, i.e., the rupturing (lysis) of red blood cells (erythrocytes). The hemolysis rate of PCL/GEL, PVA/CS, PCL/GEL-PVA/CS, and PCL/GEL-PVA/CS + PL nanofibers was 9.23 ± 0.205%, 12.13 ± 0.838%, 10.02 ± 0.817, and 8.1 ± 0.69%, respectively ($p < 0.001$).

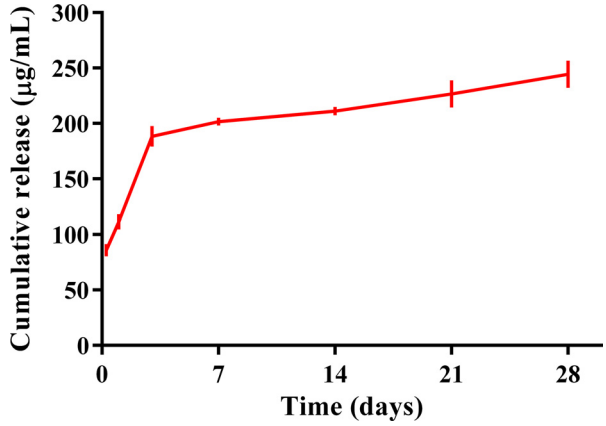

Figure 5. The cumulative release profile of PL from the prepared nanofibrous membrane after 6 h, 1, 3, 7, 14, 21, and 28 days of immersion in PBS.

Bacterial Penetration Activity

The capability of the nanofibrous mats in preventing bacterial penetration was well-demonstrated, and the outcomes are presented in Table 3. As reported, the samples exhibited a significant potential

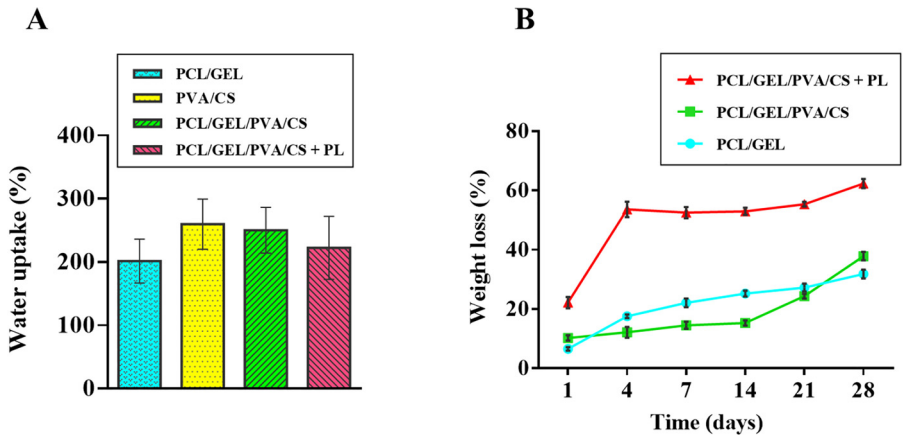

Figure 4. **(A)** The swelling properties of nanofibrous membranes (PCL/GEL, PVA/CS, PCL/GEL-PVA/CS, and PCL/GEL-PVA/CS + PL) after 24h immersion in PBS. **(B)** The percentage of nanofibers' weight loss (PCL/GEL, PCL/GEL-PVA/CS, and PCL/GEL-PVA/CS + PL) after 1, 4, 7, 14, 21, and 28 days' post-incubation in PBS. The data are indicated as mean ± standard deviation (SD), $n = 3$.

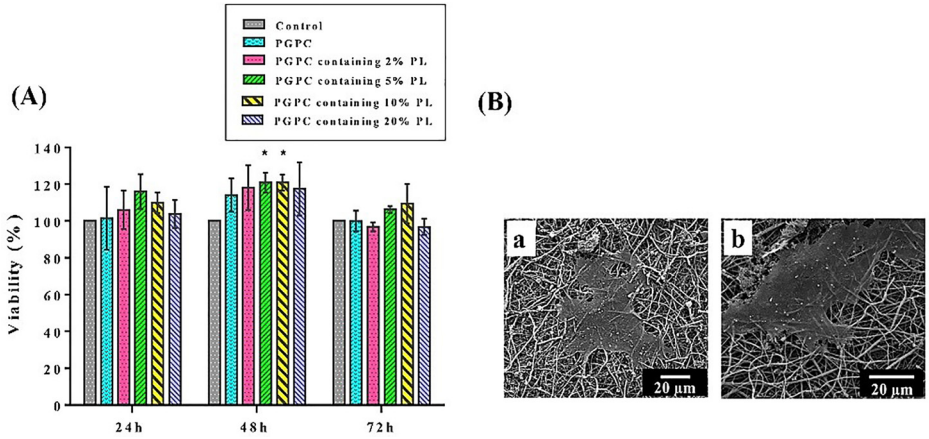

Figure 6. **(A)** The viability (%) of NIH 3T3 cells exposed to nanofibrous membranes containing 0, 2, 5, 10, and 20% PL compared to the control group (untreated cells) at 24, 48, and 72h post-incubation. Data are expressed as mean ± standard deviation (SD), $n = 3$, and $^{*}p < 0.05$ compared to the control group. **(B)** The FESEM micrographs of cell attachment onto the surface of nanofibrous membranes (a) without or (b) with PL.

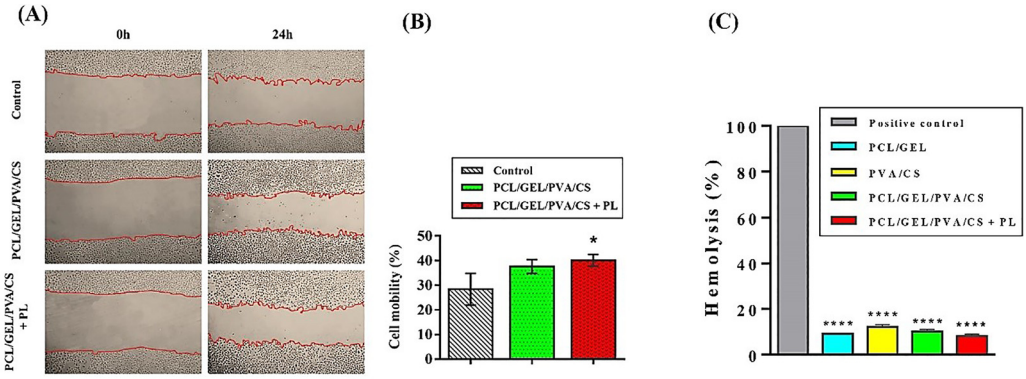

Figure 7. **(A)** Microscopic images of *in vitro* scratch assay of the untreated HUVECs and or treated with the nanofibrous scaffolds after 24h. In each image, the leading edges are plotted in red. **(B)** Quantitative graph demonstrating the percentage of HUVEC mobility after 24h. The results are shown as mean ± standard deviation (SD), $n = 6$, and $^{*}p < 0.05$ compared to the control. **(C)** The percentage of hemolysis of different experimental nanofibrous membranes (i.e., PCL/GEL, PVA/CS, PCL/GEL-PVA/CS, and PCL/GEL-PVA/CS + PL) compared to the positive control. The data are shown as mean ± SD, $n = 3$, and $^{****}p < 0.001$ compared to the positive control.

of preventing bacterial penetration in comparison with the positive control (the open test tubes without any caps) ($p < 0.001$).

Discussion

Epithelialization is a critical step of wound healing, which directly affects the success rate of skin repair and regeneration. The absence of re-epithelialization augments the risk of infection and wound recurrence.[13] Of great importance is that the early application of proper wound coverage can avoid bacterial infection as well as support epidermal cell migration, adhesion, and proliferation. In this sense, electrospun nanofibers have emerged as appropriate dressings to promote wound healing and subsequent wound closure due to their high surface to volume ratio as well as desired porosity, which allows for great drug encapsulation, excess exudate absorption, preventing bacterial invasion and infection, and efficient gaseous exchange.[2] Historically, the utilization of composite nanofibrous scaffolds made of both natural and synthetic polymers has led to providing more imitation of native skin ECM in terms of morphology and composition.[14] On the other side, the topical application of platelet derivatives can be considered as a promising approach for improving the quality and rate of the wound healing process.[15] PL, as a natural rich cocktail of various GFs and cytokines, can be easily achieved by simple thermal cycles of PRP.[16] Removal of platelet debris via gradient centrifugation makes PL a better alternative to the PRP due to lower immunogenicity. Therefore, it can be considered as a potential therapeutic in allografts or xenografts.[17,18] PL has been successfully applied for local treatment of non-healing ulcers.[19] Moreover, it has been stated that PL could enhance wound closure by triggering the early migratory potential of keratinocytes.[9] In addition to having various GFs, PL can also play pivotal roles in efficient chronic wound healing by releasing different pro-inflammatory cytokines and antimicrobial peptides.[9] However, local injection of PRP or PL was associated with prompt leakage, the short half-life of soluble components, and denaturation. Hence, several PL-containing biomaterials are being evaluated in order to promote the stability and bioactivity of PL including PL-incorporated hydrogels[20] and nanofibrous scaffolds.[8]

Table 3
The Percentage of Microbial Penetration Across the Nanofibrous Mats During 7 and 14 Days.

Samples	Day 7	Day 14
PCL/GEL	0.34 ± 0.031%	0.044%
c-PVA/CS	0.048 ± 0.00693%	0.14 ± 0.015%
c-PCL/GEL-PVA/CS	0	0.057 ± 0.02%
c-PCL/GEL-PVA/CS+PL	0	1.%2 0.0359%

The present study aimed to prepare composite nanofibers made of both natural (gelatin and chitosan) and synthetic (PCL and PVA) polymers for potential use in epidermal regeneration. As shown in Fig 1, the fibrous mats have a randomly oriented morphology with fiber diameters of 1134 ± 314 and 279 ± 50 nm for PCL/GEL (Fig. 1A and 1H) and PVA/CS (Fig. 1B and 1I), respectively. Simultaneous electrospinning of the two polymeric solutions led to the formation of nanofibers with an average diameter of 454 ± 257 nm (Fig. 1D and 1K). It is well-documented that the topical application of PRP can be considered as a promising candidate for improving the quality and rate of the wound healing process.[21-23] PL, as a natural rich cocktail of various GFs and cytokines, can be easily achieved by simple thermal cycles of PRP.[16] Removal of platelet debris via gradient centrifugation makes PL a better alternative to the PRP due to lower immunogenicity. The addition of 5% (w/w) PL to PCL/GEL-PVA/CS solution resulted in more homogenous fiber diameter. This effect can be related to the increased fiber diameter of PVA/CS + PL nanofibers (Fig 1F and M). It should be mentioned that the crosslinking of the fabricated scaffolds with 0.5% (v/v) of glutaraldehyde vapor had no significant effect on fiber composition, diameter, and morphology.

FTIR spectra of the fabricated nanofibers revealed the presence of characteristic bands of all four constituent polymers, which supports the blended nature of nanofibrous mats (Fig. 2). The FTIR spectrum of all samples showed bands at 600-700 cm^{-1} due to vibration bending of C—H, C—O stretching at 1000-1320 cm^{-1}, N=O at 1500-1600 cm^{-1}, C=O at 1695-1705 cm^{-1}, symmetric CH_2 stretching at 2868, and asymmetric CH_2 stretching at 2939.[24] In addition, PCL/GEL, PVA/CS, and c.PVA/CS nanofibrous mats demonstrated absorption bands related to stretching vibration of N—O at 940-980 cm^{-1}. A slightly sharp peak corresponding to N—H was also observed at 600-700 cm^{-1} in the blended composite nanofibers of PCL/GEL-PVA/CS, PCL/GEL-PVA/CS + PL, and their cross-linked nanofibrous mats. The addition of PL to the nanofibrous mats led to an absorption peak at 1600-1700 cm^{-1}, which can be associated with the amino characteristic peak (Fig. 2f and g). It has been previously proved that amides represent the most intense absorption bands in proteins and proteins-containing compositions (e.g., PL).[25] The presence of the crosslinker (i.e., glutaraldehyde) can be also seen in the FTIR spectrum as to a slight shift to a lower wavenumber and changing the transmittance intensity (Fig. 2c, 1e, and g). The reason behind shifting the FTIR spectrum to lower/higher wavenumber may be related to internal ordering, generation of the new bonds, and creation of the surface defects in the samples.[26,27] The existence of a shift in the FTIR spectrum to lower wavenumbers in the cross-linked samples could be associated to the interaction of glutaraldehyde with the macromolecule polymers and/or remaining of the residual crosslinker in the process. In this sense, as can be observed in Fig. 2, carbon- and nitrogen-bearing bonds including C—H, C—O, C=O, and N—O bands shifted to lower wavenumbers.

The mechanical properties of the fabricated nanofibrous scaffolds are shown in Fig. 3 and Table II. According to the data, the addition of PCL/GEL nanofibers to the PVA/CS nanofibrous system significantly increased the UTS and E from 0.69 to 1.23 MPa, and from 0.57 to 3.61 MPa, respectively. As shown in Table 2, the recorded values of UTS, E, and final strain for the nanofibrous mats were significantly increased after crosslinking with glutaraldehyde (0.5 % v/v). As it can be found, the addition of PL to the blended system resulted in an increased elongation and reduced E. Our findings are in line with previously reported studies that state these events may be associated with enhanced deformation of the nanofibrous structure after incorporation of PL.[8] It is generally suggested for a biomimetic scaffold to have mechanical properties similar to the target tissue in order to support a better tissue restoration. Based on the literature,[28] the highest and lowest E values in the human being belong to submandibular skin (1.28 MPa ±0.06) and forearm skin (1.03 MPa ±0.06), respectively. These values are in the range of elastic modulus of nanofibrous mats fabricated in our study. Accordingly, the fabricated nanofibrous scaffolds have great potential for being used in wound dressing applications.

The hydrophilicity of nanofibrous scaffolds plays important roles in cellular performance, including cell adhesion, proliferation, and migration.[29,30] The hydrophilicity of nanofibrous scaffolds was measured using the water contact angle test. It is well-established that the contact angle relies on two major parameters; i.e., the chemical composition of the substrate and the solid-liquid interactions of the surface.[31] As it is obvious in Fig. 1 Supplementary, all the samples have a hydrophilic nature with a contact angle of 0° after 5 seconds. However, there was a slight difference in the rate of the water absorption of the different groups. The maximum water contact angle is assigned to the PCL/GEL nanofibers which were 146° at the moment of dripping and 60° after 2 seconds (Fig. 1 Supplementary). Although, the other samples immediately absorbed the water after 2 seconds, suggesting the great hydrophilicity of the fabricated nanofibers. Moreover, the swelling capacity of nanofibers is an important factor to provide moisture [32] as well as absorbing excess exudate during wound healing. As shown in Fig. 4 A, all the samples indicated a high potential of water absorption up to more than twofold of their initial dry weight. This considerable swelling capacity could be attributed to the hydrophilic functional groups within the polymeric composition, including hydroxyl (OH), amine (NH_2), amide (CONH, $CONH_2$), and hydrogen bonds.[29] In addition to water uptake, the weight loss of nanofibers plays an important role during tissue regeneration due to their critical roles in supporting cell proliferation and migration as well as newly deposited ECM. Furthermore, the dissolution rate has a direct impact on releasing the incorporated therapeutic agents. As observed in Fig. 4B, the PCL/GEL and PCL/GEL-PVA/CS nanofibrous scaffolds were degraded gradually in a time-dependent manner up to 31.823 ± 1.467% and 37.85 ± 1.447% after 28 days, respectively. However, the addition of PL to the PCL/GEL-PVA/CS nanofibrous mats resulted in a sharp increase in weight loss at 4 days post-incubation in PBS medium (53.613 ± 2.607% *vs.* 12.141 ± 1.829% related to the PCL/GEL-PVA/CS nanofibers). Then the dissolution rate of PCL/GEL-PVA/CS + PL nanofibrous mats mildly increased until reaching 62.377 ± 1.51% after 28 days. This burst initial weight loss may be related to the incorporation of PL into the nanofibrous mats due to its hydrophilic nature that can make it more soluble in the PBS.[8] This durability and wettability of the fabricated nanofibers in our study suggest that these constructs can be removed from the wound bed after re-completion of epithelialization.

The release kinetics of PL from the nanofibrous mats in PBS was evaluated after 6 h, 1, 3, 7, 14, 21, and 28 days. As demonstrated in Fig. 5, PL has a burst release in the first 3 days (from 85.8 ± 5.659 μg/mL after 6 h to 188.357±9.163 μg/mL after 3 days), which is followed by a controlled and prolonged release up to 28 days (up to 244.28± 12.311 μg/mL). As reported elsewhere,[33] PL can be considered as a rich source of various GFs, cytokines, and other bioactive molecules (TGF-β1, PDGF-BB, VEGF, HGF, FGF-2, EGF, IGF-1, and KGF) which can accelerate the wound healing process. Prior experimental studies have clarified the positive effects of the sustained release of PL from nanofibrous scaffolds in skin repair and regeneration. For instance, PVA nanofibrous mats loaded with PL were shown to have a relatively high biodegradability that limits the prolonged release of bioactive molecules from the scaffold.[34] The polymeric constituents of the present study can overcome these limitations by increasing the durability of nanofibrous mats through the blended mixture of various polymers with different weight-loss rates. In addition, it has been reported that chitosan can serve as a suitable carrier for platelet's bioactive molecules and stabilizes them during blending.[35] Currently, it is accepted that any tissue-engineered construct must have compatibility with living systems like mammalian cells. Fig. 6 A indicates that

all the prepared nanofibers have no toxic effects on NIH-3T3 fibroblasts after 1, 2, and 3 days of incubation. Importantly, the incorporation of PL with the final concentrations of 2, 5, 10, and 20% (w/w) to the nanofibrous mats increased the viability and proliferation of the cells (Fig. 6 A). However, we selected 5% (w/w) PL-containing samples for further investigations due to their better outcomes in terms of cell viability after 48h ($p < 0.05$). This observation may be correlated to the burst release of PL during the first 4 days. In addition to cell proliferation and migration, efficient cell adhesion to the underlying substrate is critical for successful wound healing.[36] Since the nanofibers showed appropriate cytocompatibility, it was almost predictable that the cells can grow onto the fabricated samples. Fig. 6 B displays the SEM micrographs of the cell-laden nanofibrous mats after 5 days of seeding. As it can be seen, the cells were well attached and proliferate on the nanofibers' surface. Our data is inconsistent with previously reported experiments that state the bone marrow-derived mesenchymal stem cells (BM-MSCs) could successfully attach and infiltrate into the PRP-containing PCL/GEL nanofibrous scaffold.[37]

In addition to enhanced cell growth and proliferation, the wound closure depends on the migration of cells located at the wound edges. In our study, the adding of PL to the nanofibers could obviously augment HUVEC mobility (Fig. 7 A and B), which may positively impact accelerated neovascularization and wound closure *in vivo*.

In addition to the cytocompatibility of the fabricated nanofibers, we investigated their blood compatibility. It is well-documented that hemolysis occurs as a consequence of disruption of the erythrocyte membrane, leading to the release of hemoglobin into the plasma. This phenomenon can directly influence the blood compatibility of any material and substance.[38] As shown in Fig. 7 C, the PCL/GEL, PVA/CS, PCL/GEL-PVA/CS, and PCL/GEL-PVA/CS + PL electrospun mats exhibit a hemolysis rate of 9.23 ± 0.205%, 12.13 ± 0.838%, 10.02 ± 0.817, and 8.1 ± 0.69%, respectively, which is significantly lower than the positive control (distilled water) ($p < 0.001$). It should be highlighted that prior experiments state the lower hemolysis rate for PCL/GEL mats containing cinnamon as compared to a positive control group (distilled water).[39] The results of bacterial penetration across the electrospun mats (Table 3) proved that the fabricated nanofibers are suitable constructs for wound coverage due to their capability of preventing bacterial invasion and possible secondary infection of the wound. This observation may be due to electrostatic interactions between amine groups of chitosan and PL with the surface negative charge of bacteria, which can protect the wound bed against bacterial infection.[40] Furthermore, the nanoscale pore size of electrospun scaffolds was mentioned to be efficiently hinder bacterial transition across the nanofibrous mats.[41,42]

Conclusion

Despite considerable progress in skin tissue engineering, it seems that less attention has been paid to developing epidermal substitutes. Accordingly, we fabricated a series of electrospun nanocomposites by using PCL, GEL, PVA, and CS, in which PL was included for generating a wound dressing with high therapeutic potential. The fabricated PCL/GEL-PVA/CS + PL nanofibrous mats revealed appropriate physico-chemical properties in terms of submicron diameters, hydrophilicity, swelling, weight loss, as well as drug release profile. The obtained results clarified that the scaffolds can not only serve as a biocompatible and biomimetic substrate for cell growth and proliferation but also as a drug delivery vehicle for sustained release of bioactive molecules. Additionally, the PL-containing scaffolds have exhibited excellent compatibility with blood and could prevent bacterial invasion. All in all, the obtained data makes great proof for conducting further *in vivo* studies in order to comprehensively evaluations of the scaffolds in terms of skin tissue engineering.

Conflict of Interest

The authors declare no conflict of interest regarding the publication of this work

Acknowledgments

This project has been kindly supported by Mashhad University of Medical Sciences through research Grant No 991894.

Supplementary Materials

Supplementary material associated with this article can be found in the online version at doi:10.1016/j.xphs.2022.04.008.

References

1. Proksch E, Brandner JM, Jensen JM. The skin: an indispensable barrier. *Exp Dermatol*. 2008;17(12):1063–1072.
2. Nazarnezhad S, Baino F, Kim H-W, Webster TJ, Kargozar S. Electrospun nanofibers for improved angiogenesis: promises for tissue engineering applications. *Nanomaterials*. 2020;10(8):1609.
3. Nemati S, Kim S-j, Shin YM, Shin H. Current progress in application of polymeric nanofibers to tissue engineering. *Nano convergence*. 2019;6(1):1–16.
4. Lu H-T, Huang G-Y, Chang W-J, et al. Modification of chitosan nanofibers with CuS and fucoidan for antibacterial and bone tissue engineering applications. *Carbohydr Polym*. 2022 119035.
5. ElMessiry M, Fadel N. The tensile properties of electrospun poly vinyl chloride and cellulose acetate (PVC/CA) bi-component polymers nanofibers. *Alexandr Eng J*. 2019;58(3):885–890.
6. Fahimirad S, Abtahi H, Satei P, Ghaznavi-Rad E, Moslehi M, Ganji A. Wound healing performance of PCL/chitosan based electrospun nanofiber electrosprayed with curcumin loaded chitosan nanoparticles. *Carbohydr Polym*. 2021;259: 117640.
7. Ehrmann A. Non-toxic crosslinking of electrospun gelatin nanofibers for tissue engineering and biomedicine—a review. *Polymers*. 2021;13(12):1973.
8. Cordenonsi LM, Faccendini A, Rossi S, et al. Platelet lysate loaded electrospun scaffolds: Effect of nanofiber types on wound healing. *Eur J Pharm Biopharm*. 2019;142:247–257.
9. Backly RE, Ulivi V, Tonachini L, Cancedda R, Descalzi F, Mastrogiacomo M. Platelet lysate induces in vitro wound healing of human keratinocytes associated with a strong proinflammatory response. *Tissue Eng Part A*. 2011;17(13-14):1787–1800.
10. Ranzato E, Patrone M, Mazzucco L, Burlando B. Platelet lysate stimulates wound repair of HaCaT keratinocytes. *Br J Dermatol*. 2008;159(3):537–545.
11. Losi P, Al Kayal T, Buscemi M, Foffa I, Cavallo A, Soldani G. Bilayered fibrin-based electrospun-sprayed scaffold loaded with platelet lysate enhances wound healing in a diabetic mouse model. *Nanomaterials*. 2020;10(11):2128.
12. Liang CC, Park AY, Guan JL. In vitro scratch assay: a convenient and inexpensive method for analysis of cell migration in vitro. *Nat. Protoc*. 2007;2(2):329–333.
13. Rousselle P, Braye F, Dayan G. Re-epithelialization of adult skin wounds: cellular mechanisms and therapeutic strategies. *Adv Drug Deliv Rev*. 2019;146:344–365.
14. Chen S, Liu B, Carlson MA, Gombart AF, Reilly DA, Xie J. Recent advances in electrospun nanofibers for wound healing. *Nanomedicine*. 2017;12(11):1335–1352.
15. Nie J, Zhang S, Wu P, Liu Y, Su Y. Electrospinning with lyophilized platelet-rich fibrin has the potential to enhance the proliferation and osteogenesis of MC3T3-E1 cells. *Front Bioeng Biotechnol*. 2020:1388.
16. Fekete N, Gadelorge M, Fürst D, et al. Platelet lysate from whole blood-derived pooled platelet concentrates and apheresis-derived platelet concentrates for the isolation and expansion of human bone marrow mesenchymal stromal cells: production process, content and identification of active components. *Cytotherapy*. 2012.
17. Lucchini G, Introna M, Dander E, et al. Platelet-lysate-expanded mesenchymal stromal cells as a salvage therapy for severe resistant graft-versus-host disease in a pediatric population. *Biol Blood Marrow Transplant*. 2010;16(9):1293–1301.
18. Chevallier N, Anagnostou F, Zilber S, et al. Osteoblastic differentiation of human mesenchymal stem cells with platelet lysate. *Biomaterials*. 2010;31(2):270–278.
19. Lykov A, Surovtseva M, Bondarenko N, Kim I, Smagin M, Poveshchenko O. *Platelet Lysate and Non-Healing Ulcers*. 2020.
20. Jooybar E, Abdekhodaie MJ, Alvi M, Mousavi A, Karperien M, Dijkstra PJ. An injectable platelet lysate-hyaluronic acid hydrogel supports cellular activities and induces chondrogenesis of encapsulated mesenchymal stem cells. *Acta Biomater*. 2019;83:233–244.
21. Akhundov K, Pietramaggiori G, Waselle SD, et al. Development of a cost-effective method for platelet-rich plasma (PRP) preparation for topical wound healing. *Annals Burns Fire Disast*. 2012;25(4):207.
22. Oneto P, Etulain J. PRP in wound healing applications. *Platelets.*. 2021;32(2):189–199.
23. Carter MJ, Fylling CP, Parnell LK. Use of platelet rich plasma gel on wound healing: a systematic review and meta-analysis. *Eplasty*. 2011;11.

24. Dou Y, Fa X, Gu Y, et al. Fabrication and characterization of PVA/CS-PCL/gel multiscale electrospun scaffold: simulating extracellular matrix for enhanced cellular infiltration and proliferation. *J Biomater Sci Polym Ed*. 2020;31(6):729–746.
25. Gautam S, Dinda AK, Mishra NC. Fabrication and characterization of PCL/gelatin composite nanofibrous scaffold for tissue engineering applications by electrospinning method. *Mater Sci Eng*. 2013;33(3):1228–1235.
26. Kermani F, Mollazadeh S, Kargozar S, Vahdati Khakhi J. Improved osteogenesis and angiogenesis of theranostic ions doped calcium phosphates (CaPs) by a simple surface treatment process: a state-of-the-art study. *Mater Sci Eng C*. 2021;124:112082.
27. Kargozar S, Milan PB, Amoupour M, et al. Osteogenic potential of magnesium (Mg)-doped multicomponent bioactive glass: in vitro and in vivo animal Studies. *Materials (Basel)*. 2022;15(1).
28. Griffin M, Leung B, Premakumar Y, Szarko M, Butler P. Comparison of the mechanical properties of different skin sites for auricular and nasal reconstruction. *J Otolaryngol-Head Neck Surg*. 2017;46(1):1–6.
29. Sheik S, Sheik S, Nairy R, et al. Study on the morphological and biocompatible properties of chitosan grafted silk fibre reinforced PVA films for tissue engineering applications. *Int J Biol Macromol*. 2018;116:45–53.
30. Fathollahipour S, Abouei Mehrizi A, Ghaee A, Koosha M. Electrospinning of PVA/chitosan nanocomposite nanofibers containing gelatin nanoparticles as a dual drug delivery system. *J Biomed Mater Res Part A*. 2015;103(12):3852–3862.
31. Ashraf SS, Parivar K, Roodbari NH, Mashayekhan S, Amini N. Fabrication and characterization of biaxially electrospun collagen/alginate nanofibers, improved with Rhodotorula mucilaginosa sp. GUMS16 produced exopolysaccharides for wound healing applications. *Int J Biol Macromol*. 2021.
32. Sheik S, Sheik S, Nairy R, et al. Study on the morphological and biocompatible properties of chitosan grafted silk fibre reinforced PVA films for tissue engineering applications. *Int J Biol Macromol*. 2018;116:45–53.
33. Daikuara LY, Yue Z, Skropeta D, Wallace GG. In vitro characterisation of 3D printed platelet lysate-based bioink for potential application in skin tissue engineering. *Acta Biomater*. 2021;123:286–297.
34. Filova E, Blanquer A, Knitlova J, et al. The Effect of the Controlled Release of Platelet Lysate from PVA Nanomats on Keratinocytes, Endothelial Cells and Fibroblasts. *Nanomaterials*. 2021;11(4):995.
35. Bhatnagar P, Law JX, Ng S-F. Chitosan Reinforced with Kenaf Nanocrystalline Cellulose as an Effective Carrier for the Delivery of Platelet Lysate in the Acceleration of Wound Healing. *Polymers*. 2021;13(24):4392.
36. Anjum F, Agabalyan NA, Sparks HD, Rosin NL, Kallos MS, Biernaskie J. Biocomposite nanofiber matrices to support ECM remodeling by human dermal progenitors and enhanced wound closure. *Sci Rep*. 2017;7(1):1–17.
37. Liu J, Nie H, Xu Z, et al. Construction of PRP-containing nanofibrous scaffolds for controlled release and their application to cartilage regeneration. *J Mater Chem B*. 2015;3(4):581–591.
38. Song X, Li T, Cheng B, Xing J. POSS–PU electrospinning nanofibers membrane with enhanced blood compatibility. *RSC Advances*. 2016;6(70):65756–65762.
39. Salehi M, Niyakan M, Ehterami A, et al. Porous electrospun poly (ε-caprolactone)/gelatin nanofibrous mat containing cinnamon for wound healing application: in vitro and in vivo study. *Biomed Eng Lett*. 2020;10(1):149–161.
40. Salehi M, Naseri-Nosar M, Azami M, Nodooshan SJ, Arish J. Comparative study of poly (L-lactic acid) scaffolds coated with chitosan nanoparticles prepared via ultrasonication and ionic gelation techniques. *Tissue Eng Regenerat Med*. 2016;13(5):498–506.
41. Fahimirad S, Fahimirad Z, Sillanpää M. Efficient removal of water bacteria and viruses using electrospun nanofibers. *Sci Total Environ*. 2021;751: 141673.
42. Lanno G-M, Ramos C, Preem L, et al. Antibacterial porous electrospun fibers as skin scaffolds for wound healing applications. *ACS Omega*. 2020;5(46):30011–30022.